

1 West Nile Virus spread in Europe - 2 phylogeographic pattern analysis and key 3 drivers

4 Lu Lu^{1,13*}, Feifei Zhang^{1,12,13}, Bas B. Oude Munnink², Emmanuelle Munger², Reina S.
5 Sikkema², Styliani Pappa³, Katerina Tsioka³, Alessandro Sinigaglia⁴, Emanuela Dal Molin⁴,
6 Barbara B. Shih⁵, Anne Günther⁶, Anne Pohlmann⁶, Martin Beer⁶, Rachel A. Taylor⁷,
7 Frederic Bartumeus^{8,9,10}, Mark Woolhouse¹, Frank M. Aarestrup¹¹, Luisa Barzon⁴, Anna
8 Papa³, Samantha Lycett⁵, Marion P. G. Koopmans²

9

10 1 Usher Institute, University of Edinburgh, Edinburgh, United Kingdom

11 2 Erasmus MC, Viroscience and Pandemic and Disaster Preparedness Centre, Rotterdam, the
12 Netherlands

13 3 Department of Microbiology, Medical School, Aristotle University of Thessaloniki,
14 Thessaloniki, Greece.

15 4 Department of Molecular Medicine, University of Padova, Padua, Italy

16 5 Roslin Institute, University of Edinburgh, Edinburgh, United Kingdom

17 6 Institute of Diagnostic Virology, Friedrich-Loeffler-Institut, Greifswald-Riems, Germany

18 7 Department of Epidemiological Sciences, Animal and Plant Health Agency, United Kingdom

19 8 Centre for Advanced Studies of Blanes (CEAB-CSIC), Girona, Spain.

20 9 Centre for Research on Ecology and Forestry Applications (CREAF), Barcelona, Spain

21 10 Catalan Institution for Research and Advanced Studies (ICREA), Barcelona, Spain

22 11 Research Group for Genomic Epidemiology, Technical University of Denmark, Kongens
23 Lyngby, Denmark

24 12 Present address: National Institute of Health Data Science at Peking University, Beijing,
25 China

26 13 These authors contributed equally: Lu Lu, Feifei Zhang

27 * Email: lu.lu@ed.ac.uk

28

29

30 Abstract

31 Spread and emergence of West Nile virus (WNV) in Europe have been very different from
32 those observed in North America. Here, we describe key drivers by combining viral genome
33 sequences with epidemiological data and possible factors of spread into phylodynamic models.
34 WNV in Europe has greater lineage diversity than other regions of the world, suggesting
35 repeated introductions and local amplification. Among the six lineages found in Europe, WNV-
36 2a is predominant, has spread to at least 14 countries and evolved into two major co-circulating
37 clusters (A and B). Both of these seem to originate from regions of Central Europe. Viruses of
38 Cluster A emerged earlier and have spread towards the west of Europe with higher genetic
39 diversity. Amongst multiple drivers, high agriculture activities were associated with both
40 spread direction and velocity. Our study suggests future surveillance activities should be
41 strengthened in Central Europe and Southeast European countries, and enhanced monitoring
42 should be targeted to areas with high agriculture activities.

43 **Keywords:** West Nile virus; Europe; Phylodynamics; Phylogeography; Drivers of
44 transmission; Disease ecology; Molecular epidemiology

45 Introduction

46 Mosquito-borne viruses represent a considerable public health problem worldwide, causing
47 infections in both humans and animals¹. For the European region, West Nile virus (WNV) is
48 one of the mosquito-borne viruses which can cause severe disease and death in humans and
49 has been increasing in prevalence and geographic range over the past decade². WNV belongs
50 to the family *Flaviviridae* (genus *Flavivirus*) with an enveloped, single-stranded RNA genome
51 ³. The transmission cycle of WNV involves mosquitos (mainly of the *Culex* species) as vectors
52 and birds as amplifying reservoir hosts⁴, while humans and other mammals are considered
53 dead-end hosts¹. Dead-end hosts are not thought to contribute significantly to transmission in
54 the natural life cycle of the virus. However, for humans, the potential for virus transmission
55 through blood transfusion and organ transplantation has impacted blood and transplantation
56 donor programs, with mandatory screening for regions where exposure to WNV is possible.
57 Currently nine distinct lineages (WNV-1 to WNV-9) of WNV have been identified globally,
58 but little is known about their phenotypic properties⁵. WNV-1 and WNV-2 strains have been
59 identified most frequently in human and animal cases in multiple continents, while strains
60 within WNV-3 to WNV-9 have been detected from mosquitos, birds and equines sporadically
61 in parts of Europe, Asia, and Africa⁶. The dominant lineage in Europe in recent years is WNV-
62 2, although cases of WNV-1 have been reported^{7,8}.

63

64 WNV circulation in Europe was first reported in the 1960s⁹. Since 1996, an increasing number
65 of WNV outbreaks in humans and equines were detected in Southeast and Central Europe¹⁰. In
66 past decades, WNV outbreaks in humans and animals have been found almost annually in
67 previously non-endemic areas¹¹. As surveillance and clinical testing of WNV infections are
68 patchy, it is difficult to compare case notifications across Europe. Nevertheless, considerable
69 differences have been observed between successive years, with for instance particularly severe

70 regional WNV outbreak involving both humans and equids in 2018¹² detected in Italy, Serbia,
71 and Greece¹³. Since the beginning of the 2022 transmission season, over 60 outbreaks among
72 birds (mainly in Italy) have been reported and over 800 human cases of WNV infections were
73 reported in seven countries, mainly in Greece and Italy⁷. Unlike in the United States, where the
74 initial WNV (WNV-1) incursion in 1999 led to rapid dispersal of the virus throughout the
75 continent¹⁴, patterns of spread have remained somewhat patchy in Europe and involved both
76 WNV-1 and WNV-2. Although there have been studies on the presence and the spread of WNV
77 in different European countries¹⁵⁻¹⁷, the overall dispersal history and the important drivers have
78 yet to be determined. Therefore, we explored the possible added value of integrated analysis
79 of different types of publicly available and newly acquired data to understand and potentially
80 predict the trajectory of WNV dispersal across Europe.

81

82 To infer the virus dispersal history from sequence and other data, it is important to model how
83 viruses are dispersed through space, between species or host-types. For inference of
84 transmission patterns of viruses between discrete locations, a phylogenetic discrete traits
85 analysis can be used¹⁸. If the dispersal history of viruses is in a continuous space setting¹⁹, the
86 coordinates of the ancestral nodes of the tree could be inferred from the sampled locations and
87 two-dimensional diffusion rate¹⁹. The inferred transmission pattern between locations and the
88 spreading rate can be further modelled as functions of a combination of spatial environmental
89 factors, and the contribution of the factors modulating the transmission pattern can be
90 determined²⁰. In addition, the importance of factors which may affect the viral effective
91 population size (a measure of the extend of circulation inferred from sequence diversity) over
92 time can be estimated using a Generalized Linear Model (GLM) approach based on the
93 temporal data (for example, seasonal or climate change signals)²¹. In addition, increased virus

94 transmission rates and dispersal are signals of changing outbreak potential, although drivers
95 for spread during outbreaks and drivers of incursion to new regions might differ.

96

97 In this study, we explored the dispersal history of WNV in Europe and the underlying drivers
98 in regions with yearly WNV outbreaks and in regions with sporadic outbreaks. We used
99 phylodynamic models which incorporated: (i) sequencing data (Supporting file 1), (ii)
100 epidemiological data (host species, sampling time and coordinates, as well as travel history of
101 humans if available) (Supporting file 1), (iii) socio-economic data (population and GDP), and
102 (iv) environmental data (climatic, land cover, land use, biodiversity) (Supporting file 2 and 3).
103 Updated sequencing data and epidemiology data were provided by a European collaborative
104 consortium initiated by a group of experts across Europe (<https://www.veo-europe.eu/>).
105 Specifically, we described the evolution and genetic diversity of WNV in Europe; we then
106 explored the pattern of transmission between and within countries and the possible predictors
107 of spread.

108 Results

109 Diverged WNV lineages found in Europe

110 We found a positive correlation between cumulative human cases in EU/EEA reported by
111 ECDC (between 2008-2021, total n=4188) and the number of WNV-2 sequences (between
112 2004-2021, total n=485) provided from different countries ($R= 0.75$, $p<0.005$), despite the
113 varied sequencing capacity among countries (Figure S1a). Among the 22 European countries
114 that have human cases reported, 15 of them have sequences available, including Greece, Italy,
115 Romania, Serbia, Hungary, Spain, Austria, France, Bulgaria, Germany, Netherlands, Slovenia,
116 Portugal, Slovakia and Czechia; sequences are missing from six countries (Croatia, Kosovo,
117 Albania, Bosnia and Herzegovina, North Macedonia, Montenegro, and Cyprus) in the east

118 region (Figure S1b). By comparing the number of sequences available versus the number of
119 human cases reported, the sequencing effort in central and north regions are better than the
120 south and east regions (Figure S1b).

121

122 The maximum likelihood tree of all available WNV genome sequences showed that six
123 lineages (out of the total 9 lineages globally²²) were detected in Europe⁶ (Figure 1). Among the
124 six lineages, WNV-2 had the largest number of sequences available, accounting for 82% of all
125 WNV sequences detected in Europe so far, and the widest diffusion, since it has been found in
126 15 European countries (Figure S2). The earliest WNV-2 genome (JX041631.1) was sampled
127 from birds in Eastern Europe (Ukraine) in 1980 (Figure 1b and 1c). The dominant sub-lineage
128 2a (WNV-2a) emerged in 2004 and became the dominant lineage in the past ten years, while
129 the other lineages were rarely seen in the same time period. In addition, there was a separate
130 small sub-lineage 2b (WNV-2b) composed of sequences mainly from Romania, Italy and
131 Russia in 2011-2015, and one detection in Greece in 2018²³ (Figure 1b and S2).

132

133 In comparison, sequences of the second largest lineage (WNV-1) have been found in seven
134 European countries (Austria, Italy, Spain, France, Hungary, Romania and Portugal) since 1971.
135 Most WNV-1 sequences were reported in Italy (72% of total WNV-1 sequences), including all
136 currently available WNV-1 sequences from humans. WNV sequences belonging to lineages 3,
137 4, 8 and 9 were only sporadically reported and all of them were collected from mosquitoes:
138 WNV-3 strains were only found in Czech Republic in 1997 and 2006; WNV- 4 in Romania in
139 2012-13; WNV-8 were only found in Spain in 2006, while WNV-9 genomes were obtained in
140 Austria in 2013 and Hungary in 2011 (Figure 1c,1d and Figure S2). In addition, up to 2021,
141 these lineages (WNV-1, 3, 4, 8 and 9) were only collected from non-human hosts (mainly birds

142 or mosquitos, very few equines), except 9 WNV-1 genomes from humans in Italy between
143 2009-2013.

144

145 [Phylodynamics of the predominant WNV-2a](#)

146 Considering the distinct genetic diversity, the number of sequences available, and the
147 dominance of WNV-2 as cause of human disease, the detailed phylodynamic analyses were
148 focused on WNV-2a. These sequences were collected from 14 countries between 2004 to 2021,
149 with most available sequences from Greece (n=64), Italy (n=50), and Germany (n=46)
150 (Supporting file 1). The sequences were collected from 6 host types, with 30% from bird, 30%
151 from mosquito and 40% from humans and mammals (Figure S3 a and b).

152 The time-scaled phylogenies of WNV-2a in Europe rooted with the first genomes found in
153 Hungary, with the estimated time to the most recent common ancestor (TMRCA) dated back
154 to July 2003, with a 95% highest posterior density (HPD) interval between November 2002
155 and July 2004. The WNV-2a sequences in Europe were split into two distinct sub-clusters (A
156 and B) on the tree composed of full genome sequences (Figure 1a), which were previously
157 named the central eastern clade and southeastern clade, respectively (Figure 2a). We could see
158 that the two clusters evolved independently after the incursion from central Europe. Both
159 Cluster A and Cluster B are present in Serbia, Slovakia, Hungary, Slovenia and Italy. Cluster
160 A has also been transmitted to Austria, Czech Republic, Germany, the Netherlands, France and
161 Spain; while Cluster B has also been found in Greece, Romania and Bulgaria.

162

163 Next, we estimated the time of emergence and rate of evolution, as well as the population
164 dynamics and speed of diffusion for the two WNV-2a clusters A and B. WNV of Cluster A
165 emerged in approximately July 2006 (with 95% HPD between January 2005 and March 2007;

166 Figure 3a). The estimated ancestor country of Cluster A was Austria, with subsequent
167 sequences identified mainly in Germany and Italy (Figure 2). With a similar evolution rate,
168 Cluster B emerged later in June 2007 (with 95% HPD between March 2006 and December
169 2008) from Hungary, and most subsequent sequences were collected from Greece (Figure 2,
170 3a and 3b).

171

172 We also compared the population dynamics of the two clusters. The effective population size
173 (N_e) of cluster A peaked around 2014, which corresponded to the expansion phase of the
174 epidemic, and then decreased slightly till the second peak at around 2018, which was consistent
175 with a high WNV activity in multiple regions. In comparison, there were less important
176 changes in N_e of Cluster B (Figure 3d). The higher genetic diversity translates into a higher
177 mean N_e of cluster A compared to Cluster B. (Figure 3d, e).

178

179 WNV-2a spread at a high diffusion rate in Europe; the estimations vary between 88 km/y (full
180 genome), 215 km/y (Ns3 gene) and 180 km/y (Ns5 gene), respectively. The dispersal velocity
181 of Cluster B sequences was higher (mean of 249 km/y with 95% HPD between 221 and 278
182 km/y using Ns3 data) than those of Cluster A (mean of 189 km/y with 95% HPD between 175
183 and 203km/y using Ns3 data) (Figure 3f and 3g). This finding is consistent with the estimation
184 of frequencies of between-countries transmissions: WNV of Cluster B tended to jump more
185 frequently among countries, with an overall number of 39 (95% HPD between 34 and 44)—
186 almost twice more often than Cluster A (Figure 3c).

187

188 [Quantified transmission frequencies between European countries and within Greece](#)

189 We quantified frequencies of transmission among the 14 European countries where we have
190 available WNV-2a sequences. We found transmissions were most likely to occur between

191 neighboring countries. In addition, Austria and Hungary (both in Central Europe) had the most
192 linkages with other countries (Figure 4 and Figure S5 and S6a).

193

194 Greece contributed the highest number of WNV-2a sequences in Europe. The time-scaled
195 analysis showed Cluster B WNV has transmitted from central Europe (Hungary) to Greece and
196 kept circulating within Greece almost annually except 2015-2016. In 2017, WNV-2a re-
197 emerged in Greece and caused outbreaks in 2018 and continued to circulate during 2019–2021.
198 Between 2017 and 2021, at least six separate introductions were observed (Figure S5). Three
199 of them were from Greece only and fell in the same group with earlier isolates from Greece
200 back to 2013. The other three groups included sequences from other countries, including
201 Hungary, Romania and Bulgaria. Among them, sequences isolated from Hungary from 2018
202 to 2019 were most closely related to sequences from Greece sampled in the same time periods.
203 This showed the possibility of both re-introduction from other countries and silent
204 circulation maintained within Greece.

205

206 The discrete trait phylogeographic analysis estimated that approximately 19 transmission
207 events between Greece and neighbouring countries occurred in the past decade. Countries that
208 had the most frequent transmissions to Greece were Hungary (n=8), followed by Serbia (n=5)
209 and Romania (n=4). The transmissions between Hungary and Greece occurred multiple times
210 between 2010 and 2019, while the transmissions between Greece and other countries occurred
211 mainly in 2012-2013. We further estimated the transmissions within Greece; between-region
212 transmissions mainly occurred in north Greece and spread to the east and south regions (Figure
213 4b and Figure S6b).

214

215 Continuous dispersal and impact of environmental factors on viral lineage dispersal

216 We reconstructed the dispersal history of WNV-2a in a continuous space (Movie S1, Figure 2
217 and 5) using a continuous phylogenetic model. WNV-2a was estimated to have originated from
218 Central Europe in 2003-2004 (Hungary). One year later, WNV-2a dispersed to the eastern part
219 of Austria and spread to the northwest and western regions (including Slovakia, Serbia,
220 Hungary, Austria, Czech Republic, Slovenia, Germany, Netherlands, France and Spain) and
221 southeastern countries (Greece, Romania, Italy, Bulgaria, Serbia, Slovakia, Slovenia). We
222 could see that WNV emerged and circulated slowly in central Europe at first, and then spread
223 to the southeast regions, and then in a westward direction. The frequency and velocity of
224 diffusion was higher in 2013-14, then slowed down, and speeded up again around 2018 (Figure
225 3f). The periods with high diffusion rates were consistent with the timing when the re-
226 emergence of WNV caused major outbreaks as well as the introduction to new geographic
227 regions, e.g., further up north spreading of WNV-2a (Cluster A) towards Germany and the
228 Netherlands.

229 We could also extract the spatio-temporal information embedded in the tree and test the
230 correlation of the phylodynamic dispersion with gridded predictors (Figure S7 and Supporting
231 file 2). We tested the impacts on dispersal directions by examining the association
232 between environmental values and tree node locations (see methods). (Figure 6 and Table S1).

233

234 Our analysis found that viral lineages tended to spread towards and remained in areas with
235 relatively high density of farming [e.g., cropland, pasture, cultivated and managed vegetation
236 (i.e., cropland and the mixture of cropland and natural vegetation), livestock count (i.e.,
237 summed sheep, pig, horse, goat, cattle, and buffalo), and mammal richness (i.e., the number of
238 mammal species for the entire class), Supporting file 2]. In addition, this analysis underlined

239 that WNV lineages were more likely to spread towards areas with high urbanization status
240 (human population density and high coverage of urban land), high coverage of wetland, as well
241 as areas with bird directive and habitats directive and flyways of Passeriformes and
242 Anseriformes. In addition to these impacts on directionality of spread, we found that the factors
243 associated with high farming density (areas with high coverage of cropland, pasture, livestock
244 count, mammal richness) may accelerate WNV dispersal velocity in Europe with strong
245 support ($BF > 20$) (Figure 7 and Table S2).

246

247 [Impact of climate/bio-diversity changes on WNV genetic diversity via time](#)

248 As the dynamics of host populations (mosquitos and birds) varies widely in different months
249 or years, it is important to understand how these variables could further affect the WNV genetic
250 diversity or population dynamics. Therefore, we examined the relationship between WNV and
251 climate change coefficients in a log-linear regression model. In this study, the covariates of
252 interest included the time-varying climate related factors (including air temperature,
253 precipitation, wind speed and direction, leaf area index) and the factors related to the trend of
254 population changes of different types of birds in Europe (Figure S8 and Supporting file 3).

255

256 We found a significant positive association between the population history of the WNV-2a and
257 the air temperature in Europe between 2004 and 2021. This concordance is supported by a
258 positive, statistically significant estimate of the coefficient relating the WNV-2a effective
259 population size to air temperature with a posterior mean of 0.18 with 95% HPD (0.08,1.68)
260 (Figure 8 and Table S3). In contrast, wind speed in the eastward direction (rather than the
261 northward direction) at a height of 10 and 100 meters above the surface of the Earth, monthly
262 total precipitation, and the trends of farmland bird populations (the change in the relative
263 abundance of 39 common bird species which are dependent on farmland for feeding and

264 nesting and are not able to thrive in other habitats) were negatively correlated, which was in
265 line with the observed data that mosquitoes were more abundant during the dry months
266 compared to the wet months. In comparison, northward wind speed and the leaf area index of
267 different types of vegetation did not have a significant impact on the genetic diversity changes
268 of WNV-2a viruses (Table S3).

269 Discussion

270 In this study, we used spatially explicit phylogeographic and phylodynamic inference to
271 reconstruct the dispersal patterns and dynamics of WNV dominant in Europe in the past twenty
272 years. Using comparative analyses of lineage dispersal statistics, we detected distinct
273 evolutionary histories of lineages WNV-1 and WNV-2 and of sublineages WNV-2a and 2b
274 within the overall spread of WNV. Although the evolution of WNV has previously been
275 examined in individual European countries in different time spans^{15,24}, this study has employed
276 a phylodynamic model to incorporate sequence data, ecological data and epidemiology data
277 and quantified the overall evolution and dispersal history across Europe. Moreover, the
278 presented analysis provided insight into the potential impact of predictors that influence WNV
279 dispersal and diversity in Europe.

280 We described how WNV is present and spreads across Europe using viral sequence data. WNV
281 in Europe has higher lineage diversity (six different lineages) compared to other regions in the
282 world, e.g., only one lineage (WNV-1) has been found in North America since 1999^{25,26}. The
283 current predominant WNV-2 (2a) sequences were only found within Europe, indicating that
284 this lineage is more likely to have emerged and circulated within Europe rather than introduced
285 via cross-continent transmissions. However, we cannot rule out the possibilities of repeated
286 introductions, due to under-sampling in non-European regions. The WNV-2a has evolved into
287 2 clusters (Cluster A and B) and spread in two directions: both originated from central Europe
288 and then spread to the west (Cluster A) and to the south (Cluster B). In recent years, the spread
289 patterns are becoming more complicated. Since 2018, WNV-2a (Cluster A) has unusually
290 spread further north even up to Germany and the Netherlands.

291

292 We highlighted that areas with high levels of agricultural activities may accelerate WNV
293 dispersal velocity as well as attract the spread direction of WNV in Europe. Meanwhile, WNV
294 is likely to spread to areas with high status of urbanization, in line with higher abundance of
295 *Culex pipens* (Figure S3 d), which prefers urban environments. A recent study suggested that
296 expansion in urbanization and demography has increased the risk of infectious disease
297 outbreaks especially in the past few decades²⁷. While other native and invasive mosquito
298 species (e.g., *Ochlerotatus caspius*, *Culex modestus*, *Aedes albopictus*, *Culex perexiguus*)
299 living in natural and agricultural environments may also play an important role as WNV vectors
300 in Europe, promoting the overwintering of WNV, especially in South and Southeast Europe
301 ^{28,29}. It is also worth noting that *Culex* hybrids from the *pipiens* and *modestus* forms have been
302 found present in Europe, which can serve as a bridge for WNV between birds and humans, and
303 the proportions of hybrids are differentially affected by temperature, e.g., 17% of *Culex* are
304 hybrids in Greece, and the figure is 6-15% in the Netherlands³⁰⁻³³. Therefore, the different
305 dynamic histories of WNV variants (WNV-2a and WNV-2b) might also be associated with the
306 presence of different mosquito species, which needs further investigation. Our observations
307 suggest that enhancing mosquito control efforts, particularly on livestock farms, may reduce
308 the rate of WNV infections; monitoring farm operations is needed to effectively mitigate
309 mosquito risk and WNV spread. In addition, the observation of the negative correlation
310 between WNV population dynamics and the declines in farmland bird species in Europe in the
311 past two decades, suggests the invasion of WNV might have an impact on the population of
312 common bird species that are dependent on farmland for feeding and nesting. Meanwhile, the
313 loss of habitat may force bird migration, increasing the possibility of WNV spreading to new
314 territories.

315

316 We found a strong relationship between the presence and movement of birds and WNV spread
317 in Europe. In terms of a natural bird reservoir, WNV sequences were obtained mainly from
318 predatory birds (35%), songbirds (20%) and captive birds (20%) (Figure S3). WNV-2a in
319 Europe spread at a high spread rate (88km/y to 218km/y) and, therefore, is more likely
320 correlated with bird movement than the travel of *Culex* mosquitos (approx.500m to 2Km/y)^{34,35}.
321 We have found that WNV may be “attracted” to areas with high coverage of bird habitats and
322 to the flyway of *Passeriformes*, particularly bird species such as the Red-backed Shrike (*Lanius*
323 *collurio*), which travels at a faster rate than WNV³⁶⁻³⁹. Therefore, our work suggested that
324 although the risk of WNV depends on both the presence of infected birds and the presence of
325 mosquitoes transmitting the disease, bird movements seed the infections into mosquito
326 populations occurring far away and introduce WNV into new regions.

327

328 In addition, climate changes in the past twenty years predicted viral genetic diversity over time.
329 We found that higher temperature is correlated with high WNV genetic diversity during the
330 entire history of WNV-2a spread in Europe. High temperature may stimulate the geographical
331 expansion of suitable arbovirus regions⁴⁰. Other epidemiological modelling studies have found
332 that mild winters and drought have been associated with WNV disease outbreaks^{40,41}. We also
333 found that precipitation and wind speed had negative correlations, which could be explained
334 by WNV infections mostly occurring during the mosquito season in summer¹ and also the dry
335 season in most European countries. In addition, we found that the direction of wind also matters,
336 as the impacts on virus genetic diversity is more likely hindered by eastward wind speed rather
337 than northward (in Europe winds coming from the south tend to be warmer). A study also found
338 that wind can affect mosquito host finding⁴².

339

340 Wild animals may have played a role in onward WNV transmissions, as antibodies were
341 detected from wild animals, such as red deer, tree squirrels and wild rodents^{43,44 45}. This
342 demonstrates that enhanced surveillance and sequencing efforts in an extended host range are
343 needed to better understand the dispersal of WNV in more diversified environments. In
344 addition, passive surveillance should focus on a range of wild birds especially predator birds
345 and passerine birds. The same applies to human surveillance. Since the early 2000s, WNV
346 circulation has been continuously monitored in some European countries with varying number
347 of human and equine cases. Surveillance of mosquitoes and birds has proven to be useful for
348 early detection of WNV circulation and identification of enzootic areas^{17,46-49}. The available
349 data do reflect enhanced efforts in some countries. In Greece, active mosquito surveillance,
350 especially in the Central Macedonia Region, is being performed since 2010 when the virus was
351 first identified in the country^{17,46,50}. In Italy, a multi-species national surveillance plan was
352 implemented since 2002, following the first WNV outbreak¹³. Arbovirus surveillance in birds
353 has been set up in the Netherlands since 2016 with the number of screened samples increased
354 each year (from n=952 in 2016 to n=7030 in 2021), although no WNV sequence was detected
355 except in 2020⁵¹, which was mostly likely transmitted from Germany, according to our
356 phylogeographic analysis. On the contrary, there is an insufficient amount of WNV genomes
357 from the Central and Southeast Europe (such as Croatia⁵², Bulgaria⁴⁷, Slovenia⁵³ as well as
358 Turkey^{54,55}) as well as Southwest (Spain⁵⁶ and Portugal⁵⁷) where WNV have been detected in
359 both humans and animals² (Figure S1). Therefore, surveillance should include more sustained
360 and collaborative efforts to fill in the gaps in WNV genomic sampling throughout Europe.

361 The risks of zoonotic diseases and their spread increase with globalisation, climate change and
362 changes in human behaviour, giving pathogens numerous opportunities to colonise new
363 territories and evolve into new forms. We used virus genomics to investigate the emergence of
364 WNV in Europe, as well as its rapid spread, evolution in a new environment and establishment

365 of endemic transmission. Most importantly, our study suggested targeted regions could deserve
366 further investigation, including areas where WNV-2a was more likely to cluster in (with high
367 urbanization and farming activities, high coverage of wetlands, as well as areas with the
368 presence and movements of migrating and resident birds) and areas with higher farming density
369 tended to accelerate the dispersal of WNV. This analysis could also be done on a more local
370 level, and with information that we have compiled, so that we could predict where WNV would
371 go in the future. Putting it into a larger perspective, our work could be extended to other
372 zoonotic pathogens and guide strategies of enhanced surveillance systems for disease
373 prevention and control.

374 Methods

375 Virus Isolation, Identification, and Genome Sequencing.

376 In this study, we included unpublished WNV-2 genomes collected from Italy (n=8) and the
377 Netherlands (n=6) between 2019 and 2021. Virus isolation, identification and sequencing are
378 as previously described ^{7,38,46}. Sequences have been submitted to GenBank with accession IDs
379 OP561452-OP561459, OP762592-OP762597 (supporting file 1).

380

381 Apart from the new WNV genomes obtained in this study, we downloaded all available
382 nucleotide sequences of WNV isolated from Europe as of 02 June 2022 from NCBI
383 (www.ncbi.nlm.nih.gov). To identify any cross-continent transmission, we blast our European
384 WNV dataset against sequences database at NCBI using Geneious Prime 2021.1.1
385 (<https://www.geneious.com>). We count in total 485 WNV sequences (from unique samples),
386 including 226 full genomes sequences. Metadata of WNV sequences were updated and
387 adjusted by this European collaborative consortium. For example, we have adjusted travel
388 history of human cases (if known) to locate the original source of infection. The coordinates of
389 samples were provided as well.

390

391 Phylodynamic reconstructions

392 Sequences were aligned with MAFFT ⁵⁸. Phylogenetic trees were first generated using IQtree
393 ⁵⁹ employing maximum likelihood (ML) under 1000 bootstraps. Sequences with >5%
394 ambiguous nucleotide sites were excluded and for sequences 100% identical to one another,
395 only one of the sequences was included. The nucleotide substitution model used for all
396 phylogenetic analyses was HKY with a Gamma rate heterogeneity among sites with four rate
397 categories. The temporal qualities of the sequence data were measured with TempEst v1.5 ⁶⁰.

398

399 We further reconstructed time-scaled phylogenies of WNV-2a, which is the predominant
400 lineage found in Europe, including all WNV-2a whole genome sequences (n=208), Ns3 gene
401 sequences (n=275), and the Ns5 gene sequences (n=232), separately (Supporting file 1). The
402 Ns3 gene dataset has the largest amount of sequences and covers the widest range of geographic
403 areas (Supporting file 1 and Figure S4). Therefore, we mainly reported the results of the
404 continuous phylogeographic analysis using Ns3 dataset in the main text. We first tested the
405 temporal signals of the ML trees generated using WNV-2a full genomes and compared these
406 results with analysis of the trees generated using NS3 and NS5 gene, respectively. The prior
407 for the evolutionary clock rate of WNV was specified with a lognormal distribution and a mean
408 of 4×10^{-4} subst/site/year with Standard Deviation of 5×10^{-4} ²⁵. Phylodynamic analyses using
409 WNV-2a sequences were conducted using time-scaled Bayesian phylogenetic methods in
410 BEAST version 1.10.4⁶⁰. The best fitted models were determined using stepping-stone
411 sampling⁶¹, which resulted in the selection of HKY+Gamma+4 substitution model—an
412 uncorrelated relaxed molecular clock model which assumes each branch has its own
413 independent rate⁶² and Skygrid⁶³ coalescent model. For each analysis, the Monte Carlo
414 Markov Chain (MCMC) was run for 10^8 steps and sampled every 10^4 steps.

415

416 We further estimated the transmissions between countries and within countries by using linked
417 parameters options in Beast to jointly estimate the between country transmissions using both
418 the Ns5 gene sequences and Ns3 gene sequences (which have different phylogenies)⁶⁰. We
419 used an asymmetric model and incorporated the Bayesian Stochastic Search Variable Selection
420 procedure (BSSVS) to identify a sparse set of transmission rates that identify the statistically
421 supported connectivity⁶⁴. We also estimated the expected number of transmissions (jumps)
422 between countries and within countries using Markov rewards⁶⁵.

423 In addition, a continuous phylogenetic diffusion model with a Relaxed Random Walk
424 extension¹⁹ was further applied to explore the geographical spread of WNV in continuous
425 space.

426 Spatial and temporal drivers of WNV dispersal

427 We tested the associations between a set of potential predictors and the dispersal events of
428 WNV using R package “seraphim”²⁰, which has been developed to study the spatio-temporal
429 phylogenies in an environmental context; it extracts the spatio-temporal information from a set
430 of phylogenetic trees and uses this information to calculate and plot dispersion statistics. We
431 prepared a list of potential predictors (n=37) which were assigned into five different groups
432 including climatic, land cover, topography, socio-economic and biodiversity (Supporting file
433 2). The predictors used in this study were adapted from our previous analysis of the drivers of
434 discovery of human infective RNA viruses⁶⁶. We also included new drivers specifically
435 relevant for arboviruses (e.g., wetland concentration, occurrence status of *Culex pipiens*)
436 (Figure S7). Resolution of predictors ranged from 30" to regional level, and all data were
437 rescaled to 0.25° where necessary. Collection of data on spatial and temporal drivers of WNV
438 dispersal and the related modelling process were performed using the R version 3.6.3 (R
439 Foundation for Statistical Computing, Vienna, Austria, 2020). For each of the potential
440 predictors, we assessed the quality of the data sources used in terms of their ability to represent
441 the underlying driver. Specifically, we assessed each driver against six characteristics using the
442 method of Horigan et al. 2022 (paper submitted) (supporting file 2). Overall, the data sources
443 were of very good quality, scoring well for accuracy, reliability and availability, including the
444 factors regarding land use which the model output as influential on WNV spread. The data for
445 *Culex pipiens* distribution was assessed to have the lowest quality amongst the factors included,
446 due to the lack of available complete data. Future work could use instead, for example, outputs
447 from Mosquito Alert (<http://www.mosquitoalert.com/en/access-to-mosquito-alert-data->

448 portal/), which has started collating reports of Culex sightings through citizen science since
449 2020. Similarly, forest-related species richness and livestock density were of lower quality;
450 livestock density was a significant factor for WNV dispersal highlighting the need for these
451 data sources to be regularly updated and ensured for accuracy.

452

453 Using these potential predictors, we can test the association between the dispersal speeds and
454 directions for each branch in the phylogenetic tree, from an ancestral node to its descendants,
455 with the equivalent paths corresponding to trajectories through the predictor maps from the
456 ancestral node locations to the descendant locations. We tested if the virus tended to remain
457 in areas with lower/higher environmental values, and/or the tendency of the lineages to disperse
458 towards lower/higher values of the predictive factors, by estimating the Bayes factor (BF)
459 comparing values explored under the inferred model with the null dispersal model simulated
460 along the tree²⁰.

461

462 We also tested the impact on diffusion rate (or dispersal duration) by examining the association
463 between dispersal durations and environmental distances computed for each branch of the tree.
464 We estimated the value Q which measures the correlation between phylogenetic branch
465 durations and environmental distances, by using the “least-cost” path model, which uses a
466 least-cost algorithm to determine the route taken between the start and end locations of
467 phylogenetic branch within the predictor raster cells⁶⁷. Following the methodology described
468 by Dellicour et al⁶⁷, for each of the environmental factors, we generated three scaled rasters by
469 transforming the original raster cell values with the following formula: $v_t = 1 + k(v_o/v_{max})$,
470 where v_t and v_o are the transformed and original cell values, respectively, and v_{max} is the
471 maximum cell value recorded in the raster. Here k ($k = 10, 100$ and 1000) is a rescaling
472 parameter that tests different strengths of raster cells relative to the conductance (positive

473 correlation) or resistance (negative correlation), with a minimum value set to "1". We
474 considered a BF value >20 as strong support for a significant correlation between the factors
475 and dispersal durations as well as dispersal directions.

476

477 We applied the skygrid-GLM model²⁷ to jointly infer the WNV effective population size along
478 with the coefficient that relates it to the covariate. This stands in contrast to post hoc approaches
479 that ignore uncertainty by comparing point estimates of the effective population size and
480 covariate values (e.g., using standard approaches for time-series comparisons). Here we
481 examine the temporal relationship between the demographic history of WNV and the climate
482 changes as well as the bio-diversity changes in Europe between 2004 to 2021 (Supporting file
483 3 and Figure S8). The temporal factors (n=22) we tested included two parts: one group was
484 climate related data obtained from ERA5 with a spatial resolution of 0.25°
485 (<https://www.ecmwf.int/en/forecasts/datasets/reanalysis-datasets/era5>) including monthly
486 values of 2m air temperature, total precipitation, northward wind speed (100m, 10m neutral,
487 and 10m); eastward wind speed (100m, 10m neutral, and 1), the leaf area index of high
488 vegetation, as well as the leaf area index of low vegetation (Supporting file 3). We also obtained
489 the common bird population index in Europe between 2004 to 2019 from The Pan-European
490 Common Bird Monitoring Scheme (PECBMS) ([https://pecbms.info/trends-and-](https://pecbms.info/trends-and-indicators/species-trends/)
491 [indicators/species-trends/](https://pecbms.info/trends-and-indicators/species-trends/)), and further grouped the data into 3 types (farmland, forest and
492 others) and bird orders (extract bird species belong to 7 bird orders that matched with the bird
493 types in our WNV sequence data: *Accipitriformes*, *Charadriiformes*, *Coliiformes*,
494 *Falconiformes*, *Galliformes*, *Strigiformes* and *Passeriformes*) independently (Supporting file
495 3).

496

Data availability

The sequence data and metadata used in these analyses are available in supporting file 1; the predictors source data are available in supporting file 2 and 3. Raw data and R code used for the analyses are available via Figshare at link <https://doi.org/10.6084/m9.figshare.21444783>

Acknowledgements

We extend a special thanks to Dr. Simon Dellicour and Dr. Mandev S. Gill from Rega Institute, for consultations of Seraphim package and skyGrid-GLM modelling.

This work is supported by European Union's Horizon 2020 research and innovation programme under Grant No. 874735 (VEO). Barbara B. Shih was partially funded by a BBSRC Core Capability Grant BB/CCG1780/1 awarded to The Roslin Institute, and SL is additionally supported by Biotechnology and Biological Sciences Research Council (BBSRC) programme grant to Roslin Institute (Award Numbers BBS/E/D/20002173)

Greece, besides VEO: supported by the EWSMD project (code 0238/5030131) in the frame of the Operational Program Competitiveness, Entrepreneurship and Innovation 2014–2020 and by EMPROS project (code 02070). The National Reference centre for Arboviruses is supported by the National Public Health Organization in Greece.

We declare that we have no competing financial, professional, or personal interests that might have influenced the performance or presentation of the work described in this article.

Author Contributions

LL, SL, A Papa, MPGK designed the study. MPGK and FMA designed the collaborative data mining project (VEO), convened the multidisciplinary partnership and provided critical input on study design and manuscript. LL, BBOM, EM, RSS, SP, KT, AS, SR, AG, A Pohlmann, MB, A Papa and LB set up sample and data collection and generated sequence data. LL and FZ were involved in collecting data on the spatial and temporal drivers of WNV dispersal. LL, FZ, SL, BBOM, RSS, BBS and RL were involved in data analysis and interpretation. LL, FZ, SL wrote the manuscript and MPGK, FB, FMA, BBOM, RSS, A Papa, MB, LB, MW provided critical feedback and contributed to manuscript editing. All authors gave final approval of the version to be published.

Competing Interests

The authors declare no competing interests

Reference

- 1 Colpitts, T. M., Conway, M. J., Montgomery, R. R. & Fikrig, E. West Nile Virus: biology, transmission, and human infection. *Clin Microbiol Rev* **25**, 635-648, doi:10.1128/CMR.00045-12 (2012).
- 2 Napp, S., Petric, D. & Busquets, N. West Nile virus and other mosquito-borne viruses present in Eastern Europe. *Pathog Glob Health* **112**, 233-248, doi:10.1080/20477724.2018.1483567 (2018).
- 3 Kramer, L. D. in *Encyclopedia of Virology (Third Edition)* (eds Brian W. J. Mahy & Marc H. V. Van Regenmortel) 440-450 (Academic Press, 2008).
- 4 Schmidt, V. *et al.* Usutu virus infection in aviary birds during the cold season. *Avian Pathol* **50**, 427-435, doi:10.1080/03079457.2021.1962003 (2021).
- 5 Rizzoli, A. *et al.* The challenge of West Nile virus in Europe: knowledge gaps and research priorities. *Euro Surveill* **20**, doi:10.2807/1560-7917.es2015.20.20.21135 (2015).
- 6 Kemenesi, G. *et al.* Putative novel lineage of West Nile virus in *Uranotaenia unguiculata* mosquito, Hungary. *Virusdisease* **25**, 500-503, doi:10.1007/s13337-014-0234-8 (2014).
- 7 Barzon, L. *et al.* Early start of seasonal transmission and co-circulation of West Nile virus lineage 2 and a newly introduced lineage 1 strain, northern Italy, June 2022. *Euro Surveill* **27**, doi:10.2807/1560-7917.ES.2022.27.29.2200548 (2022).
- 8 Garcia San Miguel Rodriguez-Alarcon, L. *et al.* Unprecedented increase of West Nile virus neuroinvasive disease, Spain, summer 2020. *Euro Surveill* **26**, doi:10.2807/1560-7917.ES.2021.26.19.2002010 (2021).
- 9 Filipe, A. R. & Pinto, M. R. Survey for antibodies to arboviruses in serum of animals from southern Portugal. *Am J Trop Med Hyg* **18**, 423-426, doi:10.4269/ajtmh.1969.18.423 (1969).
- 10 Zannoli, S. & Sambri, V. West Nile Virus and Usutu Virus Co-Circulation in Europe: Epidemiology and Implications. *Microorganisms* **7**, doi:10.3390/microorganisms7070184 (2019).
- 11 Bakonyi, T. & Haussig, J. M. West Nile virus keeps on moving up in Europe. *Euro Surveill* **25**, doi:10.2807/1560-7917.ES.2020.25.46.2001938 (2020).
- 12 Control, E. C. f. D. P. a. West Nile virus infection. *ECDC. Annual epidemiological report for 2018* (2019).
- 13 Vilibic-Cavlek, T. *et al.* Emerging Trends in the Epidemiology of West Nile and Usutu Virus Infections in Southern Europe. *Front Vet Sci* **6**, 437, doi:10.3389/fvets.2019.00437 (2019).
- 14 Lanciotti, R. S. *et al.* Origin of the West Nile virus responsible for an outbreak of encephalitis in the northeastern United States. *Science* **286**, 2333-2337, doi:10.1126/science.286.5448.2333 (1999).
- 15 Ziegler, U. *et al.* West Nile Virus Epidemic in Germany Triggered by Epizootic Emergence, 2019. *Viruses* **12**, doi:10.3390/v12040448 (2020).
- 16 Aguilera-Sepulveda, P. *et al.* West Nile Virus Lineage 2 Spreads Westwards in Europe and Overwinters in North-Eastern Spain (2017-2020). *Viruses* **14**, doi:10.3390/v14030569 (2022).
- 17 Pervanidou, D. *et al.* West Nile virus in humans, Greece, 2018: the largest seasonal number of cases, 9 years after its emergence in the country. *Euro Surveill* **25**, doi:10.2807/1560-7917.ES.2020.25.32.1900543 (2020).

- 18 Global Consortium for, H. N. & Related Influenza, V. Role for migratory wild birds in the global spread of avian influenza H5N8. *Science* **354**, 213-217, doi:10.1126/science.aaf8852 (2016).
- 19 Lemey, P., Rambaut, A., Welch, J. J. & Suchard, M. A. Phylogeography takes a relaxed random walk in continuous space and time. *Mol Biol Evol* **27**, 1877-1885, doi:10.1093/molbev/msq067 (2010).
- 20 Dellicour, S., Rose, R., Faria, N. R., Lemey, P. & Pybus, O. G. SERAPHIM: studying environmental rasters and phylogenetically informed movements. *Bioinformatics* **32**, 3204-3206, doi:10.1093/bioinformatics/btw384 (2016).
- 21 Gill, M. S., Lemey, P., Bennett, S. N., Biek, R. & Suchard, M. A. Understanding Past Population Dynamics: Bayesian Coalescent-Based Modeling with Covariates. *Syst Biol* **65**, 1041-1056, doi:10.1093/sysbio/syw050 (2016).
- 22 Fall, G. *et al.* Biological and phylogenetic characteristics of West African lineages of West Nile virus. *PLoS Negl Trop Dis* **11**, e0006078, doi:10.1371/journal.pntd.0006078 (2017).
- 23 Papa, A. *et al.* Emergence of West Nile virus lineage 2 belonging to the Eastern European subclade, Greece. *Arch Virol* **164**, 1673-1675, doi:10.1007/s00705-019-04243-8 (2019).
- 24 Chaintoutis, S. C., Papa, A., Pervanidou, D. & Dovas, C. I. Evolutionary dynamics of lineage 2 West Nile virus in Europe, 2004-2018: Phylogeny, selection pressure and phylogeography. *Mol Phylogenet Evol* **141**, 106617, doi:10.1016/j.ympev.2019.106617 (2019).
- 25 Hadfield, J. *et al.* Twenty years of West Nile virus spread and evolution in the Americas visualized by Nextstrain. *Plos Pathog* **15**, e1008042, doi:10.1371/journal.ppat.1008042 (2019).
- 26 Dellicour, S. *et al.* Epidemiological hypothesis testing using a phylogeographic and phylodynamic framework. *Nat Commun* **11**, 5620, doi:10.1038/s41467-020-19122-z (2020).
- 27 Baker, R. E. *et al.* Infectious disease in an era of global change. *Nat Rev Microbiol* **20**, 193-205, doi:10.1038/s41579-021-00639-z (2022).
- 28 Mancini, G. *et al.* Mosquito species involved in the circulation of West Nile and Usutu viruses in Italy. *Vet Ital* **53**, 97-110, doi:10.12834/VetIt.114.933.4764.2 (2017).
- 29 Fortuna, C. *et al.* Evaluation of vector competence for West Nile virus in Italian *Stegomyia albopicta* (= *Aedes albopictus*) mosquitoes. *Med Vet Entomol* **29**, 430-433, doi:10.1111/mve.12133 (2015).
- 30 Papa, A., Xanthopoulou, K., Tsioka, A., Kalaitzopoulou, S. & Mourelatos, S. West Nile virus in mosquitoes in Greece. *Parasitol Res* **112**, 1551-1555, doi:10.1007/s00436-013-3302-x (2013).
- 31 Gomes, B. *et al.* Distribution and hybridization of *Culex pipiens* forms in Greece during the West Nile virus outbreak of 2010. *Infect Genet Evol* **16**, 218-225, doi:10.1016/j.meegid.2013.02.006 (2013).
- 32 Vogels, C. B. F., Goertz, G. P., Pijlman, G. P. & Koenraadt, C. J. M. Vector competence of northern and southern European *Culex pipiens pipiens* mosquitoes for West Nile virus across a gradient of temperatures. *Med Vet Entomol* **31**, 358-364, doi:10.1111/mve.12251 (2017).
- 33 Vogels, C. B., Fros, J. J., Goertz, G. P., Pijlman, G. P. & Koenraadt, C. J. Vector competence of northern European *Culex pipiens* biotypes and hybrids for West Nile virus is differentially affected by temperature. *Parasit Vectors* **9**, 393, doi:10.1186/s13071-016-1677-0 (2016).

- 34 Ciota, A. T. *et al.* Dispersal of *Culex* mosquitoes (Diptera: Culicidae) from a wastewater treatment facility. *J Med Entomol* **49**, 35-42, doi:10.1603/me11077 (2012).
- 35 Hamer, G. L. *et al.* Dispersal of adult culex mosquitoes in an urban west nile virus hotspot: a mark-capture study incorporating stable isotope enrichment of natural larval habitats. *PLoS Negl Trop Dis* **8**, e2768, doi:10.1371/journal.pntd.0002768 (2014).
- 36 Ain-Najwa, M. Y. *et al.* Evidence of West Nile virus infection in migratory and resident wild birds in west coast of peninsular Malaysia. *One Health* **10**, 100134, doi:10.1016/j.onehlt.2020.100134 (2020).
- 37 Mancuso, E. *et al.* West Nile and Usutu Virus Introduction via Migratory Birds: A Retrospective Analysis in Italy. *Viruses* **14**, doi:10.3390/v14020416 (2022).
- 38 Rappole, J. H. & Hubalek, Z. Migratory birds and West Nile virus. *J Appl Microbiol* **94 Suppl**, 47S-58S, doi:10.1046/j.1365-2672.94.s1.6.x (2003).
- 39 Lopez, G., Jimenez-Clavero, M. A., Tejedor, C. G., Soriguer, R. & Figuerola, J. Prevalence of West Nile virus neutralizing antibodies in Spain is related to the behavior of migratory birds. *Vector Borne Zoonotic Dis* **8**, 615-621, doi:10.1089/vbz.2007.0200 (2008).
- 40 Di Pol, G., Crotta, M. & Taylor, R. A. Modelling the temperature suitability for the risk of West Nile Virus establishment in European *Culex pipiens* populations. *Transbound Emerg Dis*, doi:10.1111/tbed.14513 (2022).
- 41 Watts, M. J., Sarto, I. M. V., Mortyn, P. G. & Kotsila, P. The rise of West Nile Virus in Southern and Southeastern Europe: A spatial-temporal analysis investigating the combined effects of climate, land use and economic changes. *One Health* **13**, 100315, doi:10.1016/j.onehlt.2021.100315 (2021).
- 42 Hoffmann, E. J. & Miller, J. R. Reassessment of the role and utility of wind in suppression of mosquito (Diptera: Culicidae) host finding: stimulus dilution supported over flight limitation. *J Med Entomol* **40**, 607-614, doi:10.1603/0022-2585-40.5.607 (2003).
- 43 Garcia-Bocanegra, I. *et al.* Spatio-temporal trends and risk factors affecting West Nile virus and related flavivirus exposure in Spanish wild ruminants. *BMC Vet Res* **12**, 249, doi:10.1186/s12917-016-0876-4 (2016).
- 44 Romeo, C. *et al.* Are tree squirrels involved in the circulation of flaviviruses in Italy? *Transbound Emerg Dis* **65**, 1372-1376, doi:10.1111/tbed.12874 (2018).
- 45 Cosseddu, G. M. *et al.* Serological Survey of Hantavirus and Flavivirus Among Wild Rodents in Central Italy. *Vector Borne Zoonotic Dis* **17**, 777-779, doi:10.1089/vbz.2017.2143 (2017).
- 46 Tsioka, K. *et al.* Detection and molecular characterization of West Nile virus in *Culex pipiens* mosquitoes in Central Macedonia, Greece, 2019-2021. *Acta Trop* **230**, 106391, doi:10.1016/j.actatropica.2022.106391 (2022).
- 47 Christova, I. *et al.* West Nile virus lineage 2 in humans and mosquitoes in Bulgaria, 2018-2019. *J Clin Virol* **127**, 104365, doi:10.1016/j.jcv.2020.104365 (2020).
- 48 Papa, A., Papadopoulou, E., Kalaitzopoulou, S., Tsioka, K. & Mourelatos, S. Detection of West Nile virus and insect-specific flavivirus RNA in *Culex* mosquitoes, central Macedonia, Greece. *Trans R Soc Trop Med Hyg* **108**, 555-559, doi:10.1093/trstmh/tru100 (2014).
- 49 Sofia, M. *et al.* West Nile Virus Occurrence and Ecological Niche Modeling in Wild Bird Species and Mosquito Vectors: An Active Surveillance Program in the Peloponnese Region of Greece. *Microorganisms* **10**, doi:10.3390/microorganisms10071328 (2022).

- 50 Hadjichristodoulou, C. *et al.* West Nile Virus Seroprevalence in the Greek Population
in 2013: A Nationwide Cross-Sectional Survey. *PLoS One* **10**, e0143803,
doi:10.1371/journal.pone.0143803 (2015).
- 51 Sikkema, R. S. *et al.* Detection of West Nile virus in a common whitethroat (*Curruca
communis*) and *Culex* mosquitoes in the Netherlands, 2020. *Euro Surveill* **25**,
doi:10.2807/1560-7917.ES.2020.25.40.2001704 (2020).
- 52 Vilibic-Cavlek, T. *et al.* Emerging Trends in the West Nile Virus Epidemiology in
Croatia in the 'One Health' Context, 2011-2020. *Trop Med Infect Dis* **6**,
doi:10.3390/tropicalmed6030140 (2021).
- 53 Knap, N. *et al.* West Nile Virus in Slovenia. *Viruses* **12**, doi:10.3390/v12070720
(2020).
- 54 Ergunay, K., Bakonyi, T., Nowotny, N. & Ozkul, A. Close Relationship between
West Nile Virus from Turkey and Lineage 1 Strain from Central African Republic.
Emerging Infectious Diseases **21**, 352-355, doi:10.3201/eid2102.141135 (2015).
- 55 Erdogan Bamac, O. *et al.* Emergence of West Nile Virus Lineage-2 in Resident
Corvids in Istanbul, Turkey. *Vector Borne Zoonotic Dis* **21**, 892-899,
doi:10.1089/vbz.2021.0010 (2021).
- 56 Figuerola, J. *et al.* A One Health view of the West Nile virus outbreak in Andalusia
(Spain) in 2020. *Emerg Microbes Infect* **11**, 2570-2578,
doi:10.1080/22221751.2022.2134055 (2022).
- 57 Lourenco, J. *et al.* West Nile virus transmission potential in Portugal. *Commun Biol* **5**,
6, doi:10.1038/s42003-021-02969-3 (2022).
- 58 Katoh, K. & Standley, D. M. MAFFT: iterative refinement and additional methods.
Methods Mol Biol **1079**, 131-146, doi:10.1007/978-1-62703-646-7_8 (2014).
- 59 Minh, B. Q. *et al.* IQ-TREE 2: New Models and Efficient Methods for Phylogenetic
Inference in the Genomic Era. *Mol Biol Evol* **37**, 1530-1534,
doi:10.1093/molbev/msaa015 (2020).
- 60 Rambaut, A., Lam, T. T., Carvalho, L. M. & Pybus, O. G. Exploring the temporal
structure of heterochronous sequences using TempEst (formerly Path-O-Gen). *Virus
Evol* **2**, doi:ARTN vew00710.1093/ve/vew007 (2016).
- 61 Baele, G. *et al.* Improving the Accuracy of Demographic and Molecular Clock Model
Comparison While Accommodating Phylogenetic Uncertainty. *Mol Biol Evol* **29**,
2157-2167, doi:10.1093/molbev/mss084 (2012).
- 62 Drummond, A. J., Ho, S. Y., Phillips, M. J. & Rambaut, A. Relaxed phylogenetics
and dating with confidence. *PLoS Biol* **4**, e88, doi:10.1371/journal.pbio.0040088
(2006).
- 63 Hill, V. & Baele, G. Bayesian estimation of past population dynamics in BEAST 1.10
using the Skygrid coalescent model. *Mol Biol Evol*, doi:10.1093/molbev/msz172
(2019).
- 64 Lemey, P., Rambaut, A., Drummond, A. J. & Suchard, M. A. Bayesian
phylogeography finds its roots. *PLoS Comput Biol* **5**, e1000520,
doi:10.1371/journal.pcbi.1000520 (2009).
- 65 O'Brien, J. D., Minin, V. N. & Suchard, M. A. Learning to count: robust estimates for
labeled distances between molecular sequences. *Mol Biol Evol* **26**, 801-814,
doi:msp003 [pii]10.1093/molbev/msp003 (2009).
- 66 Zhang, F. *et al.* Global discovery of human-infective RNA viruses: A modelling
analysis. *Plos Pathog* **16**, e1009079, doi:10.1371/journal.ppat.1009079 (2020).
- 67 Dellicour, S., Vrancken, B., Trovao, N. S., Fargette, D. & Lemey, P. On the
importance of negative controls in viral landscape phylogeography. *Virus Evol* **4**,
vey023, doi:10.1093/ve/vey023 (2018).

Figures

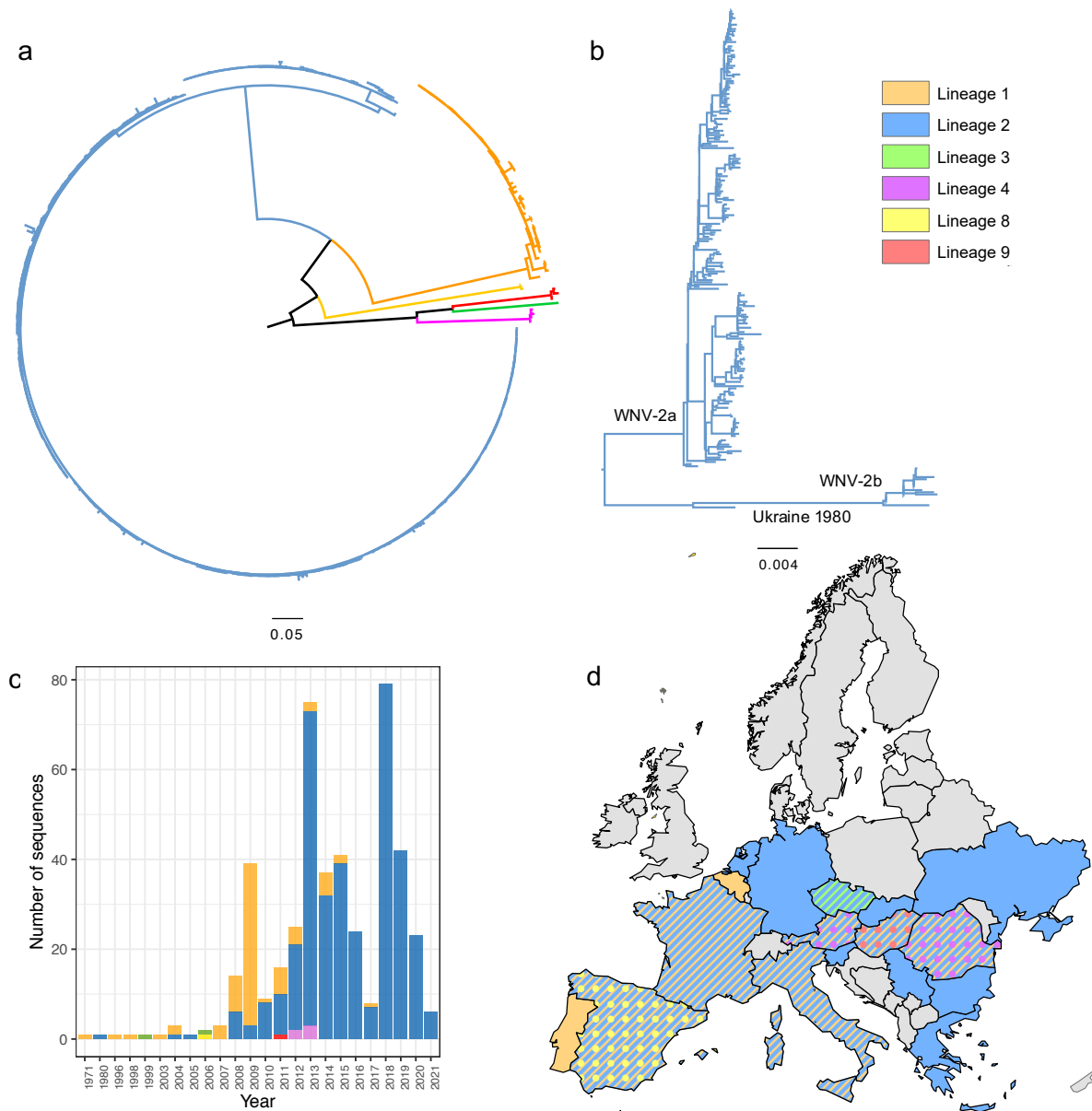


Figure 1 Phylogenetic analysis of WNV full and partial nucleotide sequences detected from Europe. The evolutionary distances were computed using the optimal GTR+I model, the phylogenetic tree was constructed with the Maximum likelihood method. Bootstrap values are given for 1000 replicates. (a) ML tree of all lineages found in Europe; the branches of the tree are colored by lineages; (b) The subtree of WNV- 2 sequences; (c) The WNV lineages distribution over time using the same color showing on the tree; (d) The geographical distribution of WNV lineages, using the same lineage color showing on the tree, and differentiate by shape if multiple lineages were found within the same country.

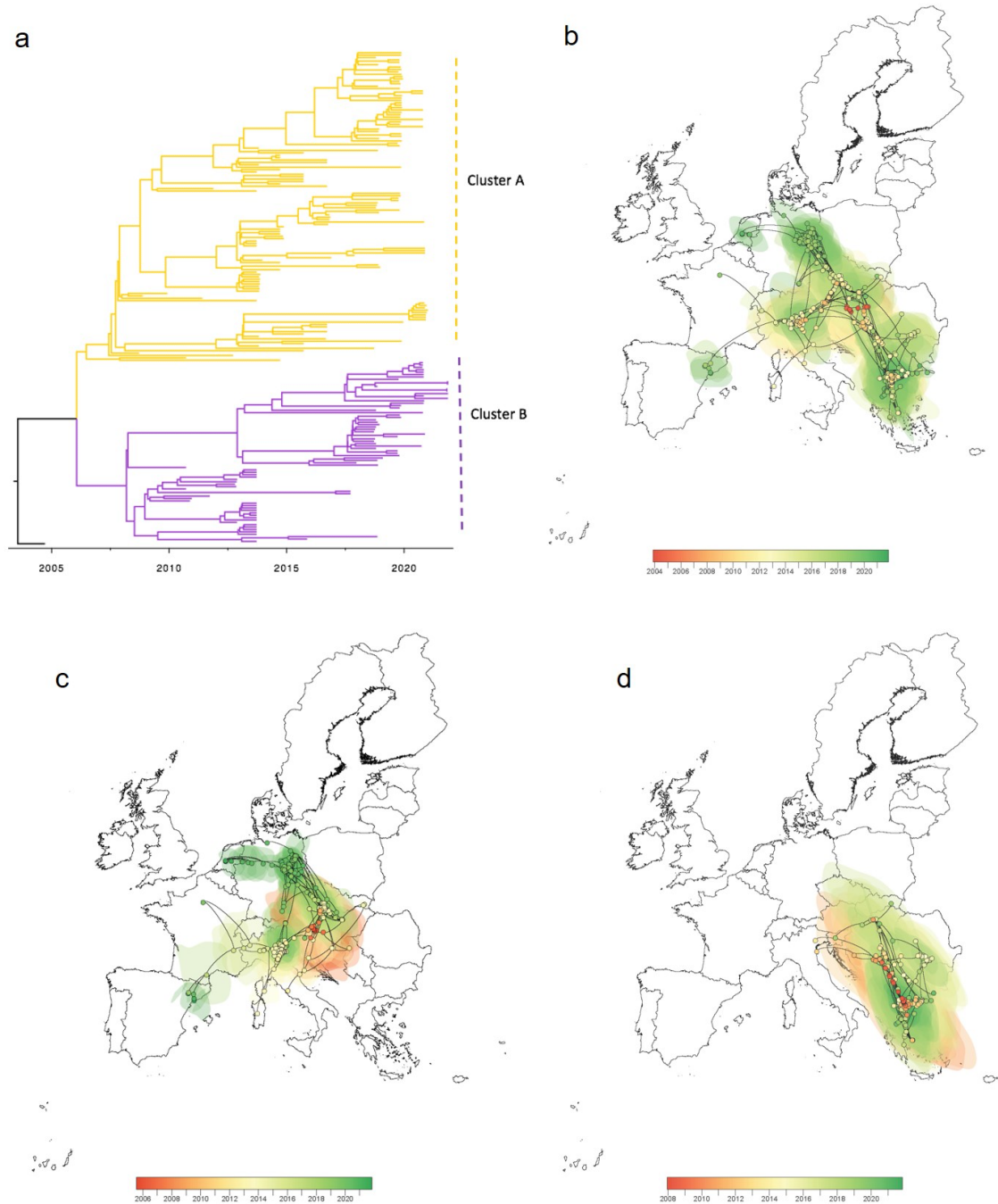


Figure 2 Time-scaled phylogeny of WNV-2a genomes in Europe. (a) Time-scaled MCC (maximum clade credibility) tree of WNV full genome sequences isolated in Europe (n=192), the two cluster A and B are labelled on the right. A distinct phylogeographic analysis has been based on Ns3 gene by continuous phylogeographic inference based on 1,000 posterior trees. Spatiotemporal diffusion of all WNV- 2a in Europe (b), of cluster A (c) and Cluster B (d). These MCC trees are superimposed on 80% the highest posterior density (HPD) interval reflecting phylogeographic uncertainty. Nodes of the trees, as well as HPD regions, are colored by timescale from red (the time to the most recent common ancestor, TMRCA) to green (most recent sampling time), and oldest nodes (and corresponding HPD regions) are here plotted on top of youngest nodes.

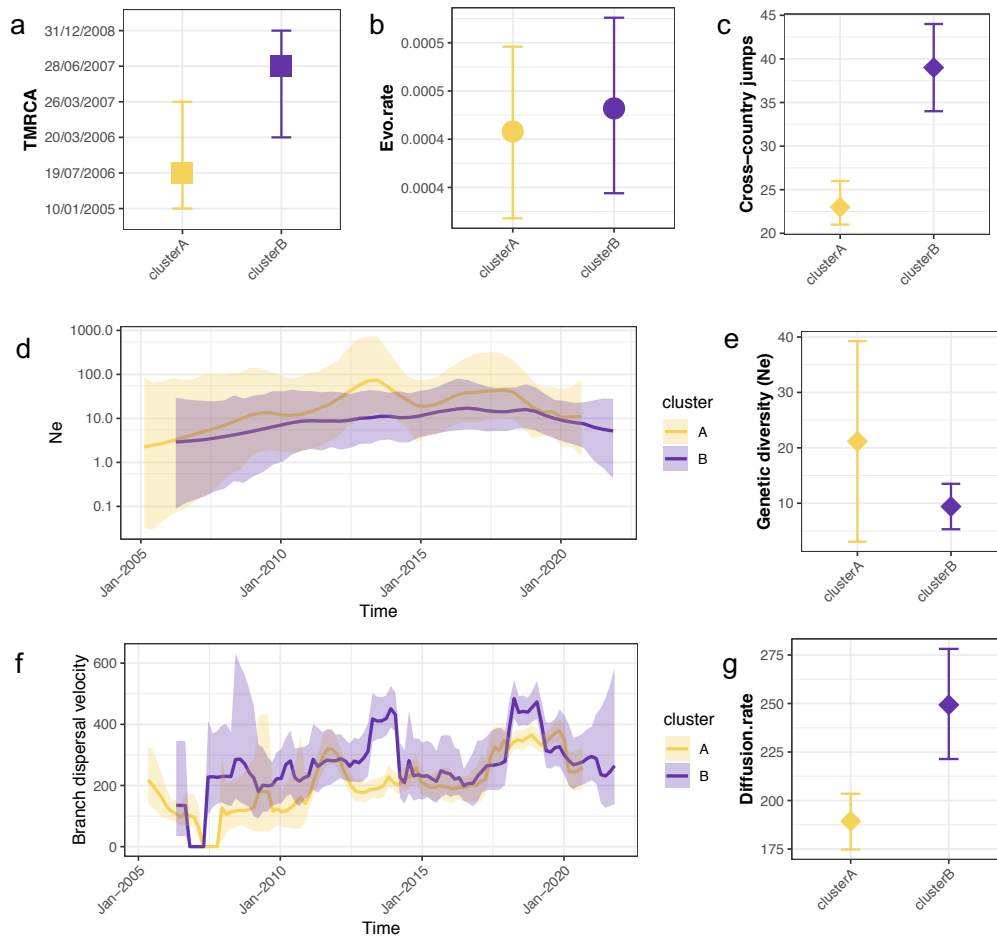


Figure 3 Comparisons of two co-circulating clusters of WNV-2a in Europe. (a) The mean time of the most recent ancestor (TMRCA) and 95%HPD interval for each cluster. (b) The mean clock rate and 95% HPD interval for each cluster. (c) Mean number of Markov jump between countries and 95%HPD interval for each cluster. (d) Estimation of effective population size via time and 95% HPD interval. The logarithmic effective number of infections (N_e) vs. viral generation time (t), representing effective transmissions is plotted over time. (e) Mean genetic diversity (N_e) and 95% HPD interval. (f) The weighted branch dispersal velocity (km/y) through time and 95% HPD interval. (g) The weighted mean diffusion rate (km/y) and 95% HPD interval.

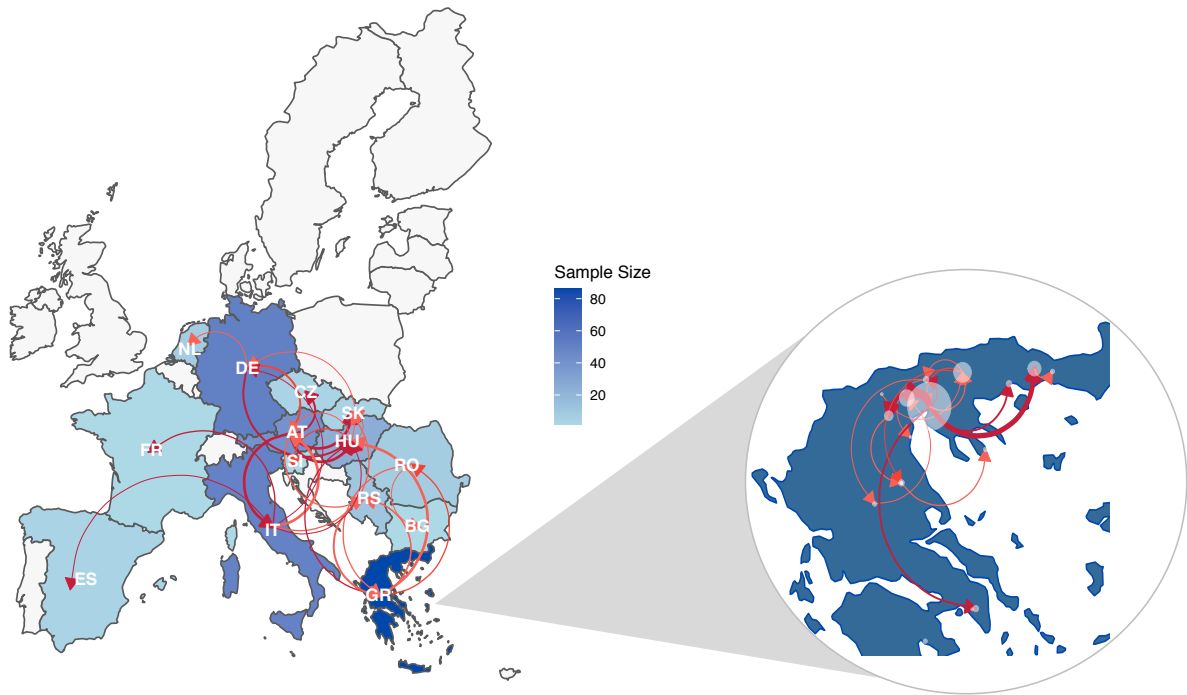


Figure 4 Quantified transmission network of WNV-2a between European countries and within Greece inferred using discrete trait models. Shape of colors on map indicates number of samples; edge weight indicates median number of transmissions between pairs of countries/regions; arrow on edge indicates transmission direction; color of edge from light to dark indicates Bayes Factor (BF) support from low to high only transmissions with $BF > 3$ are shown).

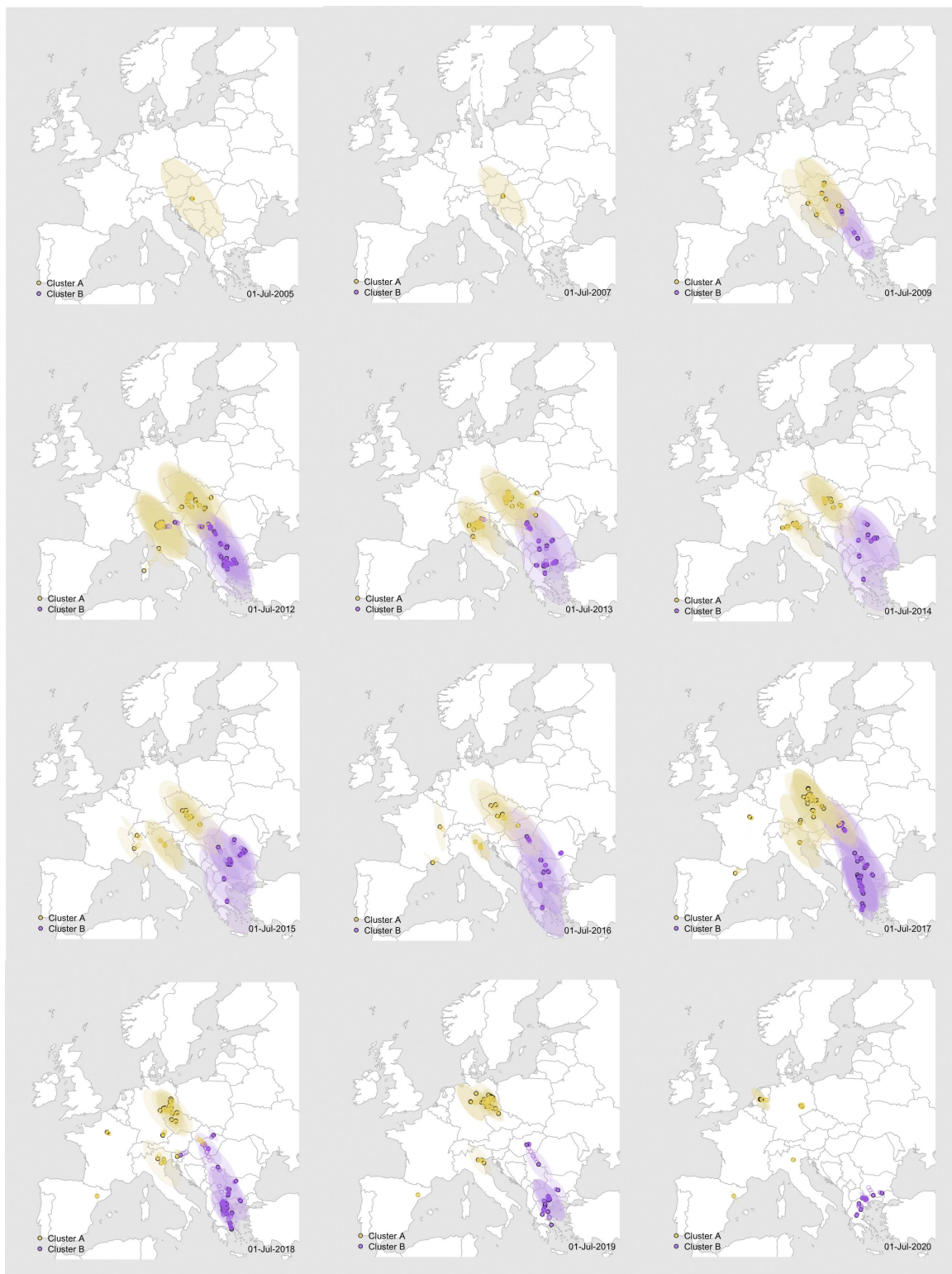


Figure 5 Dispersal history of WNV-2a in Europe between 2004 to 2021. Colors of the dots represent interpolated maximum clade credibility phylogeny positions for cluster A (yellow) and B (purple) from Ns3. Please see Movie S1 for the full movie.

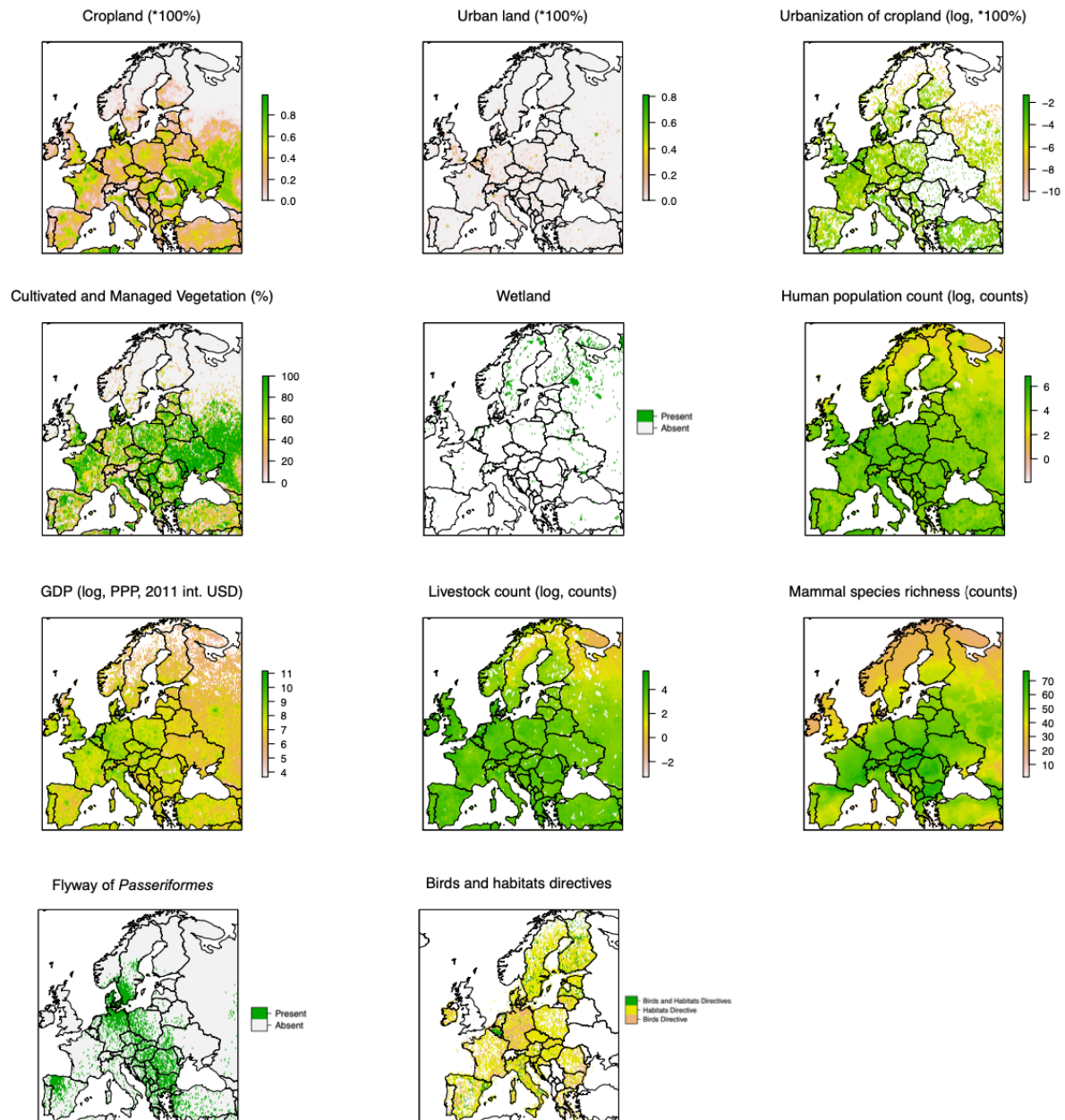


Figure 6 Explanatory factors significantly attracting WNV dispersal in Europe. There are eleven factors (out of the total 37 factors being tested) that may attract WNV dispersal with strong statistical support ($BF > 20$, as shown in Table S1). Data were log-transformed where necessary for better visualization. The visualizations and full descriptions of all factors are in Figure S7 and Supporting file 2.

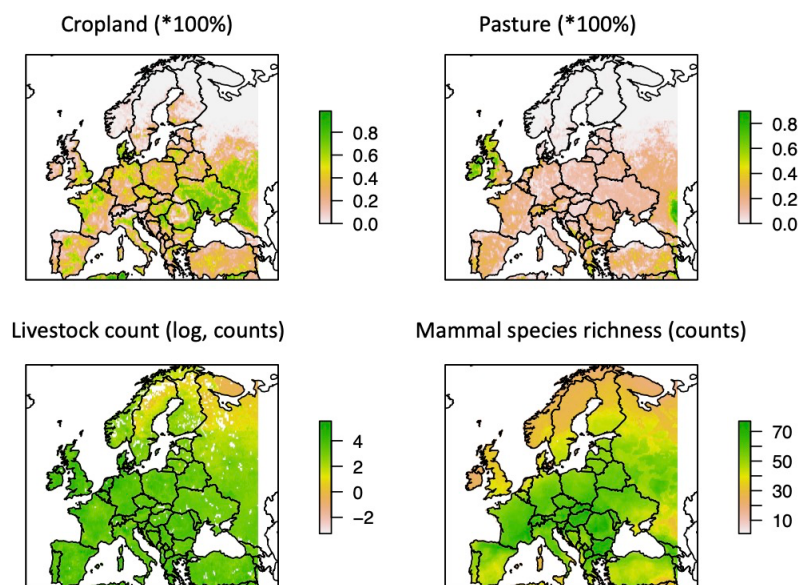


Figure 7 Explanatory factors have significant impact on WNV dispersal velocity in Europe. There are four factors (out of the total 37 factors being tested) that may speed up WNV dispersal with strong statistical support ($BF > 20$, as shown in Table S2). Data were log-transformed where necessary for better visualization. The visualizations and full descriptions of all factors are in Figure S7 and Supporting file 2.

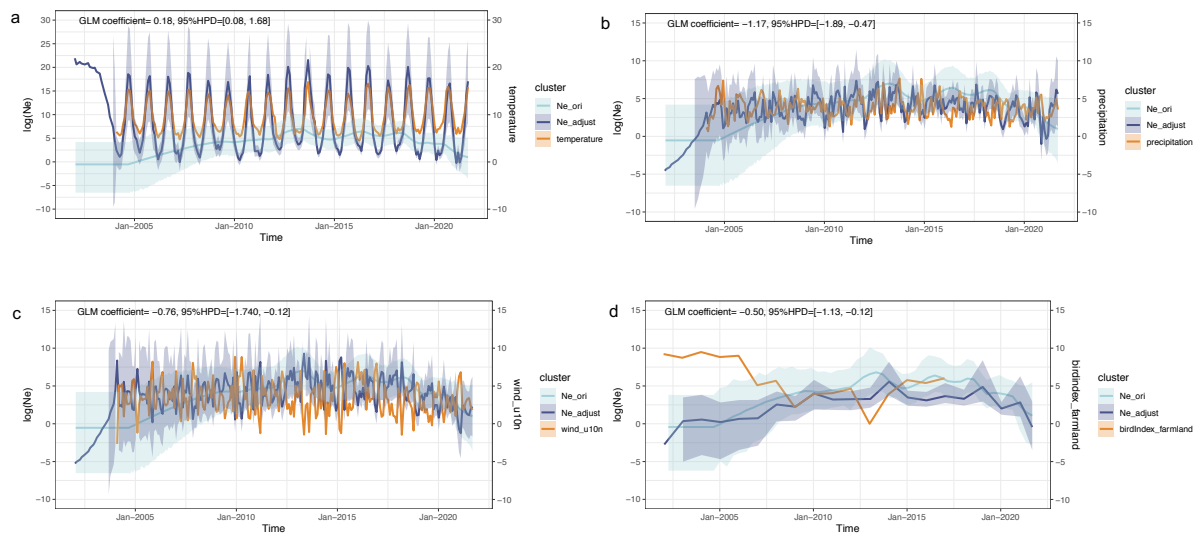


Figure 8 Time-varied factors with significant impacts on population dynamics via time. These associations were tested with a generalized linear model (GLM) extension of the coalescent model used to infer the dynamics of the viral effective population size of the virus (N_e) through time. We here present the following time-series variables as significant associated covariates (orange curves): a) mean temperature, b) mean precipitation, c) eastward wind speed at 10m, and d) the trend of farmland bird population index (measures the rate of change in the relative abundance of common bird species) between 2004 and 2019. Posterior mean estimates of the viral effective population size based on both sequence data and covariate data are represented by dark blue curves, and the corresponding dark blue polygon reflects the 95% HPD region. Posterior mean estimates of the viral effective population size inferred strictly from sequence data are represented by light blue curves and the corresponding light blue polygon reflects the 95% HPD region. A significant association between the covariate and effective population size is inferred when the 95% HPD interval of the GLM coefficient excludes zero. See the skygrid-GLM results of all factors being tested in Table S3. The visualizations and full descriptions of all factors being tested are in Figure S8 and Supporting file 3.